Differences in functional brain organization during gesture recognition between autistic and neurotypical individuals

James P. Trujillo, [1,2] Asli Özyürek, [1,2] Cornelis C. Kan, [3] Irina Sheftel-Simanova, [4] and Harold Bekkering[1]

[1]Donders Institute for Brain, Cognition, and Behavior, Donders Centre for Cognition, Nijmegen, GD 6525, The Netherlands
[2]Max Planck Institute for Psycholinguistics, Nijmegen, XD 6525, The Netherlands
[3]Department of Psychiatry, Radboud University Medical Centre, Radboudumc, Nijmegen, GA 6525, The Netherlands
[4]One Planet Research Centre, Radboud University Medical Centre, Radboudumc, Nijmegen, GA 6525, The Netherlands
Correspondence should be addressed to James P. Trujillo, Radboud University, Donders Centre for Cognition, Maria Montessori Building, Thomas van Aquinostraat 4, Nijmegen 6525 GD, The Netherlands.
E-mail: Jptrujillo88@hotmail.com.
Irina Sheftel-Simanova and Harold Bekkering contributed equally to this study.

Abstract

Persons with and without autism process sensory information differently. Differences in sensory processing are directly relevant to social functioning and communicative abilities, which are known to be hampered in persons with autism. We collected functional magnetic resonance imaging data from 25 autistic individuals and 25 neurotypical individuals while they performed a silent gesture recognition task. We exploited brain network topology, a holistic quantification of how networks within the brain are organized to provide new insights into how visual communicative signals are processed in autistic and neurotypical individuals. Performing graph theoretical analysis, we calculated two network properties of the action observation network: 'local efficiency', as a measure of network segregation, and 'global efficiency', as a measure of network integration. We found that persons with autism and neurotypical persons differ in how the action observation network is organized. Persons with autism utilize a more clustered, local-processing-oriented network configuration (i.e. higher local efficiency) rather than the more integrative network organization seen in neurotypicals (i.e. higher global efficiency). These results shed new light on the complex interplay between social and sensory processing in autism.

Key words: connectivity; graph theory; autism; fMRI; gesture

Introduction

Persons with autism spectrum conditions (ASC) process sensory information differently than those without autism (Keehn *et al.*, 2013; Van de Cruys *et al.*, 2014; Lawson *et al.*, 2017). For example, autistic individuals are often more focused on details (Bölte *et al.*, 2007) but have more difficulty filtering relevant information from noise (Van de Cruys *et al.*, 2017). These perceptual differences may relate to how prior knowledge and current sensory information are used, integrated (Pellicano and Burr, 2012) and updated (Van de Cruys *et al.*, 2014; Sapey-Triomphe *et al.*, 2020) or to the engagement and disengagement of attention in response to perceptual cues (Keehn *et al.*, 2013). Differences in sensory processing are directly relevant to social functioning and communicative abilities in ASC. For example, atypical perception of communicative manual gestures, which are a key aspect of social interaction (Kelly *et al.*, 2010; Özyürek, 2014), could lead to miscommunications. Some evidence for this link comes from

the finding that gesture recognition is strongly correlated with 'social perception' (i.e. what a person is doing, based on intonation, posture, gesture, etc.; Walther *et al.*, 2015). This study addresses the complex interplay between social and sensory processing in autism, focusing on processing of communicative gestures.

Recognition of communicative gestures provides an interesting point of investigation for autistic and neurotypical individuals because gestures are a crucial aspect of human communication (Özyürek, 2014; Holler and Levinson, 2019). Even in the absence of speech or interaction, gesture recognition is directly relevant for social functioning in that recognizing what another person is doing (i.e. whether an actual action or an action or object iconically depicted via gesture) provides the grounding to be able to effectively interact with that person (Knoblich and Sebanz, 2006). Autistic individuals may not be impaired in actually recognizing the meaning of iconic gestures (i.e. those that visually

depict an action or object; Silverman *et al.*, 2010; Trujillo *et al.*, 2021) or the referent of deictic gestures (i.e. pointing gestures; Aldaqre *et al.*, 2016; von der Lühe *et al.*, 2016), but processing may still differ between the two groups. In our previous study (Trujillo *et al.*, 2021), we found that autistic individuals recognized iconic gestures with similar accuracy as neurotypical individuals. However, autistic individuals differed in how they interpreted communicative cues in the kinematics of these gestures. This specifically related to communicatively motivated exaggerations of the kinematics, such as an increase in complexity (e.g. depicting placing a nail, then depicting the 'hammering' movement) effectively adding more depictive movements to an action or repetitiveness (e.g. repeating a 'hammering' movement) of the gestures. This kinematic exaggeration hindered autistic individuals' recognition performance rather than supporting recognition as it did in neurotypicals (Trujillo *et al.*, 2021). This finding highlights how perceptual processing differences may be quite subtle.

Besides differences in the processing of gesture kinematics, other studies have suggested that the successful processing of iconic and deictic gestures (i.e. pointing) imposes a heavier cognitive processing load than in neurotypicals (Silverman *et al.*, 2010; Aldaqre *et al.*, 2016). In other words, gesture recognition may recruit more, or different, cognitive resources in autistic compared to neurotypical persons. This may reflect a different organization of information processing or it may reflect a similar organization but generally greater mental effort in autistic individuals. While these findings relate to more complex action or gesture recognition, similar results can be seen in the recognition of biological motion from highly reduced stimuli, such as point-light displays (single points of light in the location of human joints, such as wrists and shoulders, against a black background (Johansson, 1973)). While some studies have reported impaired recognition of biological motion in autistic individuals (Blake *et al.*, 2003; Hsiung *et al.*, 2019), others have shown that there is little or no impairment (Herrington *et al.*, 2007; von der Lühe *et al.*, 2016). A recent meta-analysis suggests that any deficits may be particularly related to recognizing higher-order information, such as emotions, from biological motion alone (Todorova *et al.*, 2019). Even when behavioral performance does not differ between autistic and neurotypical individuals, patterns of brain activity and connectivity when processing biological motion do seem to differ (Herrington *et al.*, 2007; McKay *et al.*, 2012; Alaerts *et al.*, 2017). These studies demonstrate that autistic persons can be unimpaired on a particular perceptual task in terms of accuracy while the processing of the perceptual information may still be qualitatively different, and how the brain processes this perceptual information may also differ. Understanding the mechanisms underlying these differences will require us to investigate whether and how these are related to the organization of information processing in the brain.

Differences in how neurodiverse populations process (socially relevant) perceptual information will likely be reflected in how the brain responds to such information. Brain networks, and in particular the topological organization of such networks, may provide insights into such perceptual differences. This is because functional networks (i.e. the network of brain regions that are particularly active and exchanging information during a particular task) can be dynamically and flexibly organized in response to the current environment or task (Bassett *et al.*, 2006).

Studies assessing functional networks in autistic and neurotypical individuals have already provided evidence for differences between the two groups. One replicated finding is that autistic individuals have decreased long-range connectivity between different areas or networks (O'Reilly *et al.*, 2017; Hong *et al.*, 2019). However, other studies have shown increased connectivity 'between' networks, with decreased connectivity 'within' networks (Fishman *et al.*, 2014, 2015). Importantly, such differences in connectivity in autistic individuals are not only in general network organization but also occur in specific, task-relevant networks, such as the action observation network (Alaerts *et al.*, 2015, 2017; Delbruck *et al.*, 2019). The action observation network (AON), which includes the inferior frontal gyrus (IFG), posterior superior temporal gyrus (pSTG), bilateral precentral gyrus (PCG), intraparietal sulcus (IPS) and precuneus (Caspers *et al.*, 2010; Arioli and Canessa, 2019), is especially relevant as it is activated during the observation of human actions, including manual gestures (Villarreal *et al.*, 2008; Trujillo *et al.*, 2020). Differences within AON connectivity are also correlated with autism symptom severity (Delbruck *et al.*, 2019), suggesting the relevance of these network differences in social functioning. Crucially, however, all of these findings, with the exception of that of Alaerts *et al.* (2017), come from studies of resting-state connectivity, when participants are scanned without any particular task. Resting-state studies can provide an interesting view of how the brain organizes into stable patterns, but it cannot tell us how these functional networks organize during active engagement.

Investigating functional network organization during task engagement can provide us with insights into how task-related information is being processed and how this may differ between groups. As discussed above, network differences such as changes in long-range connections may be relevant in understanding how autistic individuals cognitively process information. Graph theoretical analysis provides a useful tool for understanding the architecture, or topology, of these self-organizing functional networks because it does not focus on activation differences in a specific brain area, or on particular connections, but rather on the structure of a critical network as a whole (Bullmore and Sporns, 2009; Park and Friston, 2013). This structure is relevant for cognitive processing as the balance between segregation (captured as local efficiency) and long-range integration (captured as global efficiency) is reflective of performance on several cognitive tasks (Gießing *et al.*, 2013; Cohen and D'Esposito, 2016; Farahani *et al.*, 2019). These network features, therefore, correspond well with the previously discussed results in autism, where long-range connectivity differences may be related to graph theoretical global efficiency, and more local changes may be reflected in local efficiency.

In order to better understand how autistic and neurotypical individuals differ in terms of the processing of communicative signals, the current study, therefore, assesses differences between autistic and neurotypical individuals in network topology during the recognition of silent iconic gestures. By utilizing stick-light versions of these gestures, we are able to ensure that the only information available is related to movement itself and not to the actor or further visual context. In a previous study, we reported the behavioral results from this task, where we found that autistic individuals were able to correctly recognize iconic gestures depicted by stick-light figures with similar accuracy as neurotypical individuals but differed in how they interpreted subtle differences in the kinematics of these gestures, such as the complexity or repetitiveness of the gestures (i.e. the number of submovements constituting a particular gesture). In order to understand such perceptual differences at the level of information processing in the brain, the current study compares the 'local efficiency' and 'global efficiency' of the task-related network in autistic and

neurotypical individuals. These measures characterize the segregation (higher short-range but lower long-range connectivity) and integration (higher long-range but lower short-range connectivity) of the task-related network. We focus our analyses on the AON, as this network is strongly implicated in the processing of (communicative) movements, such as hand gestures, and has previously shown to differ in terms of its internal network connectivity in autistic and neurotypical individuals. Focusing on this AON also provides a theory-driven constraint and thus improves the interpretability of the findings, while the network-based analysis overall allows us to more holistically characterize how this functional network organizes in response to this task rather than focusing on specific regions or connections. In sum, our study aims to provide new insights into how task-related brain networks organize in response to viewing and recognizing communicative gestures in both autistic and neurotypical individuals.

Methods
Participants
Twenty-five autistic individuals (15 female; 22 right-handed) and 25 neurotypical individuals (14 female; 21 right-handed) participated in the study. From the autistic group, three participants did not complete the neuroimaging part of the study due to stress or inability to lie in the scanner, and two participants were excluded postscan due to excessive head motion (see 'Preprocessing' section below). This left 20 participants in the autistic group and 24 neurotypical participants who were included in analyses. Autistic participants were recruited via the Psychiatry Department of the Radboud University Medical Centre (Radboudumc). Patients were recruited via two routes. In the first route, patients were contacted by their psychiatrist at the Radboudumc with general, global information about the study and asked if they agree to being approached by researchers. In the second route, a message was posted in a private, organization-specific social network, where Radboudumc psychiatrists have message board-style contact with past patients. All participants received a clinical diagnosis of autism spectrum disorder (ASD), also referred to as ASC, from a Radboudumc psychiatrist according to the criteria defined in the Diagnostic and Statistical Manual of Mental Disorders, Fifth addition. Diagnosis was confirmed by the psychiatrist using a structured diagnostic interview for autism (*Nederlands Interview ten behoeve van Diagnostiek Autismespectrumstoornis bij Volwassenen [Dutch Interview for the Diagnosis of Autism Spectrum Disorder in Adults]*). Participants between the ages of 18 and 35 years were recruited. Potential participants were excluded if they had a history of any other (neuro-)psychiatric disorders, brain surgery or brain trauma or used antipsychotic medication. The neurotypical control group was recruited via the Radboud University SONA system, which allows for presignup screening of several participant characteristics. By starting the recruitment of the ASC group first, we were able to prescreen our control group in an attempt to match the age and gender between the two groups. We additionally collected data on education and handedness for further group matching. The study was approved by a local ethics committee (CMO Arnhem-Nijmegen) and all procedures were performed in accordance with the Declaration of Helsinki (World Medical Association, 2013). Participants took part in a two-part study, involving gesture production and gesture comprehension. For a full description of both behavioral paradigms, see Trujillo *et al.* (2021). The power analyses used to calculate sample size are described in Appendix 1.

Sample size and power analysis
Sample size was determined based on a priori power analyses both for the analyses described here and for the behavioral measures described in Trujillo *et al.* (2021). For the current study, we utilized a previous study from our lab (Trujillo *et al.*, 2020) that similarly used stick-light figure stimuli of silent gestures during task-based functional magnetic resonance imaging (fMRI). Using the fmripower (fmripower.org; Mumford and Nichols, 2008) toolbox for Matlab, we calculated the necessary sample size to detect major AON areas, which were a priori of interest. For 80% power and a Type I error rate of 0.05, we required 25 participants. This sample size estimation was aimed at detecting the main effects of interest within-group as a sufficiently comparable dataset for performing a power analysis for between-group effects was not available. However, the current sample size estimation ensures that our design was able to elicit significant activation in the main areas of interest, on which we will perform further analyses. For the behavioral study, power analysis indicated that we needed 20 participants in each group. In order to ensure sufficient power for the entire two-part study, we, therefore, set our desired sample size at 25 per group.

Demographics and neuropsychological measures
We collected self-report information on age (years) and handedness and asked participants to fill out questionnaires for the autism quotient (AQ; Baron-Cohen *et al.*, 2001; Ketelaars *et al.*, 2008), the Actions and Feelings Questionnaire (AFQ; Williams *et al.*, 2016) and level of education (based on the highest level of completed education as defined by Verhage (Verhage, 1964) and updated by Hendriks (Hendriks *et al.*, 2014)). The AQ was collected in order to quantify autism symptom severity. The Dutch version of the AFQ (van der Meer *et al.*, 2022), which quantifies the relation between motor cognition and empathy, was collected as a secondary measure to determine if it is a valid predictor of participants' gesture recognition performance. Besides questionnaires, we also carried out the Dutch short form of the Wechsler Abbreviated Intelligence Test (WAIS-II; Wechsler, 2011), as well as the Purdue Pegboard Test (Tiffin and Asher, 1948). These were carried out in order to obtain an estimate of the intelligence quotient (IQ) and general motor coordination that could be used to ensure that the two groups are matched in these general domains.

In order to check group matching, we used equivalence testing following the two one-sided t-test (TOST) approach (Lakens *et al.*, 2018). We set the smallest effect size of interest (SESOI) for age up to 5, as age differences of less than 5 likely still fall within the same general age category. We set the SESOI for IQ to 8 following the suggestion of Lakens *et al.* (2018) to use half a standard deviation (s.d.), with an s.d. of 16 being taken from a large sample of Dutch adults performing the WAIS (van Ool *et al.*, 2018). SESOI was set to 3 for the Purdue pegboard, as this is the minimal detectable change in this test (Lee *et al.*, 2013). We used Welch's t-tests to statistically determine whether the two groups differed in the clinical scores where we expected them to differ (i.e. AFQ and AQ).

For the demographics that we expected to be matched (i.e. age, IQ and motor coordination), we found that autistic and neurotypical individuals differed significantly in age ($t(45.27) = 3.786$, $P < 0.001$) and the two groups did not differ significantly in IQ ($t(34.38) = -0.210$, $P = 0.835$), although we also did not find evidence for the groups being statistically equivalent ($t(34.38) = 1.414$, $P = 0.083$). Purdue Assembly (motor coordination) scores were statistically equivalent ($t(47.26) = -4.957$,

Table 1. Overview of demographic information

	ASC		NT	
	Mean	s.d.	Mean	s.d.
Age (years)[a]	24.08	3.72	28.67	4.78
Gender (female)	10	%50	14	%58
Handedness (right-handed)	18	%90	19	%79
Purdue Assembly (motor coordination)	9.24	1.55	9.92	1.75
IQ (estimate)	113.03	10.61	112.00	22.24
AFQ[a]	24.05	5.47	32.45	4.97
AQ[a]	30.63	7.25	14.95	6.24

ASC = autism spectrum condition; NT = neurotypical; IQ = intelligence quotient; AFQ = Actions and Feelings Questionnaire; AQ = autism quotient.
[a]Significantly different.

$P < 0.001$. For the clinical measures, we found significantly higher AFQ scores in neurotypicals compared to autistic individuals ($t(36.19) = 5.01$, $P < 0.001$), and we found higher AQ scores in the autistic individuals compared to the neurotypicals ($t(35.572) = 7.22$, $P < 0.001$). Demographic information is provided in Table 1.

Tasks and data acquisition
fMRI data acquisition
Anatomical and task-related MRI images were acquired on a 3 T Siemens Magnetom Skyra MR scanner with a 32-channel head coil at the Donders Institute for Brain, Cognition and Behaviour in Nijmegen, the Netherlands. Structural images ($1 \times 1 \times 1$ mm^3) were acquired using a T1-weighted magnetization prepared rapid gradient echo sequence with time repetition (TR) = 2300 ms, time echo (TE) = 3.03 ms, flip angle = 8° and field of view (FOV) = $256 \times 256 \times 192$ mm^3. The behavioral task (described below) was carried out by participants while T2*-weighted, multi-band 8, dual-echo echo-planar imaging (EPI) BOLD-fMRI images were acquired using an interleaved ascending slice acquisition sequence (slices = 63, TR = 730 ms, TE = 37.8 ms, flip angle = 90°, voxel size = $3 \times 3 \times 3$, slice gap = 0.34 mm, FOV = 212×212 mm^2). We additionally collected a B0-field map sequence using two magnitude images and one phase difference.

fMRI Preprocessing
We performed slice-time correction on functional images and then generated voxel displacement maps (VDM) based on the B0-field maps. These VDMs were subsequently used to unwarp the functional images. Functional and structural images were realigned and coregistered, with spatial normalization with the Montreal Neurological Institute template and spatial smoothing using a 3-mm full width at half-maximum kernel. After preprocessing, we checked motion parameters in the task-related acquisitions to ensure that no participants moved more than 3° in rotation or 3 mm in translation across the functional scanning session. This led to two autistic participants and one neurotypical participant being excluded (as noted above in the 'Participants' subsection). Given an equivalence bound of 0.102 (i.e. half the s.d. of pooled motion parameters), a TOST check indicated that the difference in motion parameters did not differ statistically between groups ($t(46.98) = -0.105$, $P = 0.917$), although not statistically equivalent ($t(46.98) = 1.644$, $P = 0.053$). All analyses were performed in MATLAB (MathWorks, Natick, MA) using SPM12.

Physical set-up
Participants were positioned in the supine position in the MRI scanner with an adjustable mirror attached to the head coil. Through the mirror, participants were able to see a projection screen outside the scanner. Participants were given an MRI-compatible response box, which they operated using the index finger of their right hand to press a button on the right and the index finger of their left hand to press a button on the left. Button locations corresponded to the two response options given on the screen. The resolution of the projector was 1024×768 pixels, with a projection size of 454×340 mm and a 755 mm distance between the participant and the mirror. The video size on the projection was adjusted such that the stick figures in the videos were seen at a size of 60×60 pixels. This ensured that the entire figure fell on the fovea, reducing eye movements during image acquisition. Stimuli were presented using an in-house-developed PsychoPy (Peirce *et al.*, 2019) script.

Stimuli
For our video stimuli, we utilized recordings from (Trujillo *et al.*, 2018). These recordings were based on a gesture production similar to what was performed in the present study, although using real objects placed in front of the participants rather than images on a computer screen. Following the same methodology of Trujillo *et al.* (2019), we utilized the motion tracking data from the 2018 recordings in order to reconstruct the movements of the upper-body joints (Trujillo *et al.*, 2018). Videos consisted of these reconstructions, using x, y and z coordinates acquired at 30 frames per second of these joints (see Figure 1 for an illustration of the joints utilized). Note that no joints pertaining to the fingers were visually represented. This ensured that hand-shape could not be used to infer the object of the enacted action being performed (Ansuini *et al.*, 2014, 2016). These points were depicted with lines drawn between the individual points to create a light stick figure, representing the participants' kinematic skeleton. These stick-light figures, while highly reduced, have previously been used in an fMRI experiment and successfully elicited activation in both biological motion and social (i.e. mentalizing) regions (Trujillo *et al.*, 2020). Skeletons were centered in space on the screen, with the viewing angle adjusted to reflect an azimuth of 20° and an elevation of 45° in reference to the center of the skeleton. This stick-light skeletons were used in order to reduce the visual information available to the participant, ensuring that the only information available was the movements of the body. In total, we utilized 120 stimuli, depicting 30 unique gestures (see Appendix 1). While specific depictions (e.g. peeling a banana and opening a lock) were repeated several times throughout the experiment, each of the 120 stimuli consisted of a unique actor–depiction combination. In other words, if 'peeling banana' appeared four times, the four instances were performed by four different participants from the (Trujillo *et al.*, 2018) study. We used this set of stick-light figures rather than, for example, more naturalistic video stimuli because this type of stimuli ensures that the main difference between videos is the kinematic qualities of the gesture rather than anything about the actors themselves. The videos also have the advantage of being unscripted. We have included a sample stimulus video in Supplementary File 1 as an example.

Task
During the task (Figure 1), participants were first presented with two response options in random order. This was the Prime phase.
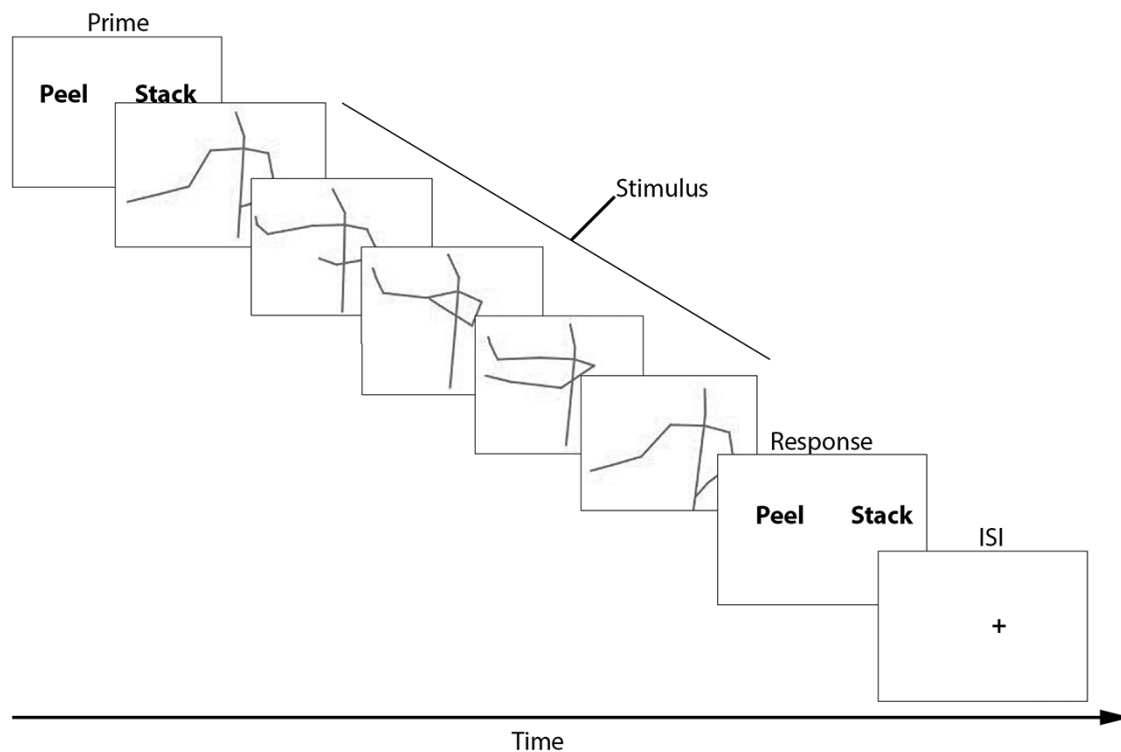
Fig. 1. Schematic overview of gesture comprehension task and stimuli. Trials start with a prime, followed by the stimulus video, after which the two response options are again shown and the participant is able to respond. After this, there is a short ISI.

After this, a stimulus video was then displayed on the screen. After this stimulus phase, the two response options were again presented on screen. The two possible answers were presented, one on the left, and one on the right. During this Response phase, participants could use a button box to pick either the left or right answer using the left and right buttons on the button box. Participants were given 2500 ms to respond. Answers consisted of one verb and one noun that captured the action (e.g. the correct answer to the item 'peel the banana' was 'peel'). Correct answers were randomly assigned to one of the two sides. The second option was always one of the possible answers from the total set. Therefore, all options were presented equally often as the correct answer and as the wrong (distractor) option. After responding, there was a variable interstimulus interval (ISI) during which participants would see a fixation cross for a period of 1000 ms with a jitter of 250 ms. See Figure 1 for a schematic overview of a trial. Accuracy and response time (RT) were recorded for each video. As this is part of a larger project, we will not discuss the analyses of the behavioral results in this paper. The main behavioral results can be found in Appendix 2 and discussed in more detail in Trujillo *et al.* (2021).

Analyses
Activation

As an initial sanity check of the data, we performed a general linear model (GLM) analysis. This allowed us to quantify general brain activation in response to the task, specifically whether theoretically expected regions would be activated, and check for any potential differences between the two groups. For this analysis, we included regressors for motion parameters, task response, ISI, prime screen, video viewing—correct, and video viewing—incorrect. The two video-viewing regressors are the main regressors of interest and relate to the total duration during which

participants were seeing the gesture video, split for videos for which a correct response was given, and videos for which an incorrect response was given.

Our main effect of interest was video viewing over baseline, taking only correct trials. This is because we were interested in which brain areas were active during accurate recognition of a gesture. After main effects analyses, which were carried out as separate contrasts for each group, we also calculated group-specific contrasts. These were ASC > NT, and NT > ASC. These contrasts allowed us to test whether activation of certain brain regions is more prominent for one group or the other. Result figures for these analyses were generated using MRIcron (Rorden and Brett, 2000).

Regions of interest

The regions chosen for subsequent analysis via graph theory approaches represent the brain areas that are typically associated with action recognition tasks (i.e. the so-called AON) as demonstrated by meta-analyses (Caspers *et al.*, 2010; Arioli and Canessa, 2019). This allows our analyses to be more focused on areas that are likely to be relevant for the task at hand. The volumetric regions of interest (ROI) for this study were implemented in the *Conn* toolbox (version 17), which utilizes a set of ROIs combining the Harvard-Oxford atlas (Desikan *et al.*, 2006) and the AAL atlas (Rolls *et al.*, 2020), which use structural parcellation rather than spherical, purely center-coordinate-based ROIs. The ROIs included in this study, and their center coordinates, were: left IFG (−51, 26,2), right IFG (54, 28, 2), left inferior parietal sulcus (IPS; −39, −43, 52), right IPS (39, −42, 54), left pSTG (−57, −47, 15), right pSTG (59, −42, 13), left PCG (−39, −6, −51), right PCG (41, −8, 52), medial prefrontal cortex (mPFC; 1, 55, −3) and precuneus (1, −61, 38). The first eight regions were selected due to their involvement in action observation, while the precuneus and

mPFC were additionally included due to their strong role in intention recognition (Enrici *et al.*, 2010; Tettamanti *et al.*, 2017; Trujillo *et al.*, 2020). Given that the kinematic characteristics of our stimuli have also been linked to social intention attribution, we had reason to believe that including these key intention processing areas would be useful for understanding the complete network of areas involved in processing socially relevant gestures.

Connectivity

While the GLM analysis provides a whole-brain overview of 'where' information is potentially being processed, connectivity analysis (our primary analysis in this study) allows us to test 'how' information is processed and moves throughout the brain. For this analysis, we used a graph theoretical approach, which treats a set of brain regions (described above) as nodes on an interconnected graph. While graph theory analyses can use any number of brain regions as nodes, we chose to focus our analysis on a set of task-relevant regions (see subsection 'Regions of interest'). At the same time, it is a more data-driven approach than methods such as psychophysiological interactions, which requires a seed region to be chosen, or dynamical causal modeling, which requires assumptions about directionality and can be computationally very intensive for larger networks. Finally, graph theoretical approaches are particularly advantageous as we are interested in information integration and local *vs* global processing based on previous autism literature.

While graph theory allows one to calculate many different metrics, we focus our analyses on two specific metrics: local efficiency and global efficiency. In graph theory, the starting point for analyses is calculating which nodes (i.e. functional brain regions) are connected. In our approach, we consider a weighted graph, meaning that connections are the correlation strength between two nodes rather than being nonweighted, where connections are binary, either connected or not. CONN specifically uses a weighted least squares linear model, with event-specific boxcar time series convolved with a hemodynamic response function in order to calculate weighted connectivity values. An important base metric in graph theory is then the path length, which describes how closely two regions are connected. For example, if information has to travel via multiple intermediary regions before reaching the other region, there is a higher path length. In weighted graphs, rather than calculating the shortest path based purely on the presence of connections, the path length is calculated by taking the inverse of the interregional connectivity values. Therefore, path length not only captures the functional distance between regions in terms of whether or not there is a direct connection but also how 'strong' this path is in terms of its connectivity values. This is because higher connectivity indicates a shorter effective 'path' between the regions. Our two measures, local and global efficiency, are directly related to the concept of path length. 'Local efficiency' is defined as the inverse of the shortest path length between a given node and all of its neighbors. Local efficiency thus captures local information integration. When applied to the entire network, local efficiency reflects the degree of local interconnectedness, with higher local efficiency suggesting that each region is connected primarily to each of its neighbors, while lower local efficiency suggests that connections are more sparsely distributed and further across the network. 'Global efficiency' is defined as the inverse of the shortest path between a node and all other nodes in the network. In contrast to capturing local integration at the level of a single node, this metric reflects the centrality or importance of the node in the

entire network. When applied to the entire network, global efficiency reflects how connected the network is as one complete system, with higher global efficiency suggesting that regions are well connected across the entire network, rather than being primarily connected at the level of neighbor-to-neighbor. Note that both measures provide a value between 0 (lowest efficiency) and 1 (highest efficiency).

The efficiency metrics are calculated using the CONN toolbox, which uses the same preprocessed data as described for the GLM analysis but additionally includes a denoising step that ensures that spurious correlations due simply to simultaneous activations in response to the same stimulus are removed (i.e. task-related fluctuations). This denoising step additionally includes 12 motion parameters (three translations, three rotations and their first-order derivatives) in order to account for motion-related BOLD activity. In both cases, denoising is performed on each subject separately. Efficiency matrices are calculated from the Fisher-transformed (Z) correlation coefficients between regions. Efficiency metrics, after being calculated in CONN, are subsequently imported into R and tested using linear mixed effects models (see next subsection).

Statistical testing of connectivity measures

For statistical testing, we take the efficiency metric (i.e. local or global connectivity) as the dependent variable, participant and ROI as random effects and group as fixed effects. Two data points were included for each participant: one for the correct trials and one for the incorrect trials. This was done to account for variation that may be due to recognizing a gesture compared to not recognizing it. Random slopes are not included, as there was insufficient data per participant for these models. Models are tested using chi-square model comparisons against a null model. This null model included the same random effects structure but did not include group as a fixed effect. A significant model comparison test would therefore indicate that group membership contributes significantly to explaining the variance in the graph metric beyond what can be attributed to baseline variation between individuals. Post hoc comparisons were calculated using the 'emmeans' package, which calculates group comparisons, per ROI, with *P*-value adjustment using Tukey's HSD.

Association between connectivity and performance on the gesture recognition task

In order to assess whether gesture recognition performance could be explained by the connectivity measures, we additionally utilized the same models described in Trujillo *et al.* (2021) for gesture recognition accuracy and RT. Namely, accuracy was modeled as $accuracy \sim video\_duration + group^*observed\_sub\ movements + (1|participant) + (1|actor) + (1|item)$, while response time was modeled as $RT \sim video\_duration + observed\_gesture\_space + observed\_submovements + group^*observed\_peak\_velocity + (1|participant) + (1|actor) + (1|item)$. Observed gesture space, submovements, and peak velocity refer to the kinematic properties of the observed gesture. For the current analysis, we used these same models but tested whether including mean local or global efficiency, with an interaction with group, significantly improved the model fit. This would suggest that brain network topology explains additional variance in task performance beyond the characteristics of the gestures themselves. We used the same chi-square model comparison described above.

Association between connectivity and neuropsychological measures

In addition to the a priori defined analyses defined above, we performed an additional exploratory test of whether the two connectivity measures are associated with relevant neuropsychological measures. To this end, we built mixed models with local or global efficiency as the dependent variable and participant and brain region as random intercepts. In three separate models, we assessed whether the model fit was improved (i.e. efficiency variance was better explained) by including AFQ score, AQ score or motor coordination (assessed by Purdue Assembly scores). We tried to fit these models with random slopes for our independent variable of interest but did not include them when this led to convergence or singularity issues. The same model comparison procedure was used as described above. In the case of significant model improvements, we additionally tested whether adding an interaction with group membership would additionally improve

the model, as this would indicate that the association between efficiency and the neuropsychological measure differed for autistic compared to neurotypical individuals. These tests were carried out based on previous reports of network connectivity being influenced by autism symptom severity (Delbruck *et al.*, 2019), as well as motor coordination being associated with activity in the AON (Kilroy *et al.*, 2021).
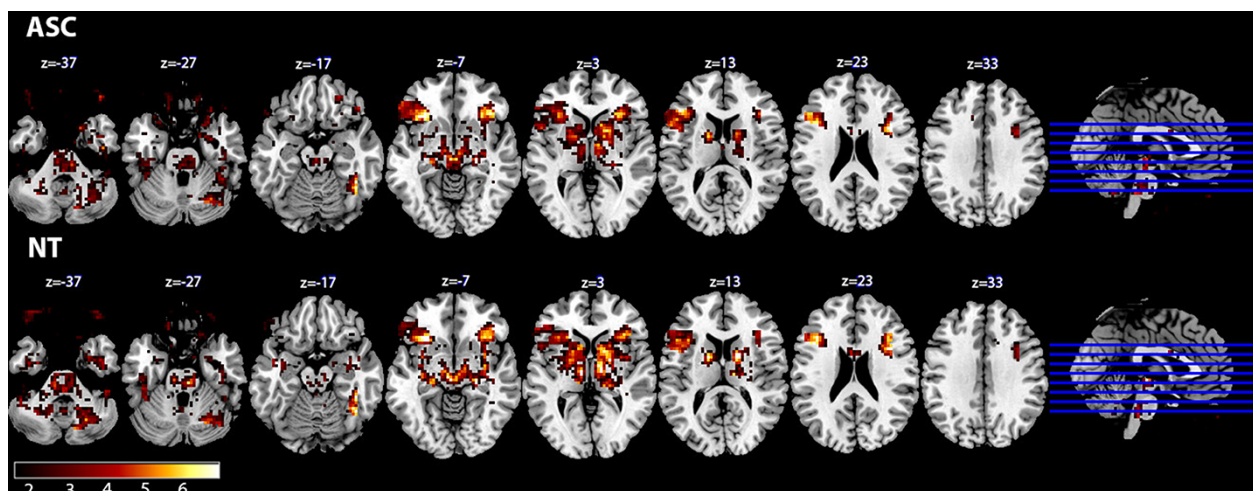
Results
Activation

The main GLM analysis tested which brain areas were significantly activated while viewing a gesture that would be correctly identified (contrast: video viewing—correct response *vs* baseline). The ASC group showed the activation of, amongst others, the bilateral IFG (BA 47), bilateral middle frontal gyrus (BA 9 and 46), as well as the caudate nucleus. The NT group similarly showed

Table 2. Overview of GLM main results, per group

L/R	BA	Region	K	t	z	X	Y	Z
ASC main effects (video viewing)								
R	9	IFG	15	10.21	7.31	39	11	23
R	13	Insula	32	8.28	6.42	33	26	−4
L	47	IFG	38	8.22	6.33	−30	23	−7
L		Cerebellum	46	7.58	6.03	−30	−73	−55
R		Cerebellum	43	7.13	5.78	27	−67	−55
R		Cerebellum	12	7.13	5.78	42	−46	−19
R	46	IFG	10	6.93	5.67	12	−10	8
L		Caudate body	35	6.85	5.62	−45	29	14
R		Thalamus	16	6.88	5.64	21	5	8
NT Main Effects (video viewing)								
R		Thalamus	54	8.77	6.63	12	−16	11
L		Cerebellum	66	8.42	6.47	−27	−70	−52
R		Cerebellum	66	8.24	6.38	12	−76	−46
L	47	IFG	33	8.16	6.33	−33	20	−4
R		Caudate Body	47	7.85	6.17	15	5	14
R	9	MFG	27	7.68	6.08	39	14	26
R	47	IFG	39	7.57	6.03	42	29	−1
L		Thalamus	32	7.51	5.99	−9	−13	5
L	46	MFG	24	7.00	5.71	−42	17	23

All results are significant at p-FWE < 0.05, k < 10. L/R = left/right; BA = Brodmann area; K = cluster size; MFG = middle frontal gyrus.

Fig. 2. Overview of GLM results, depicting results from the two groups. Colored areas indicate voxels significantly (p < 0.05 FWE corrected) associated with the video viewing *vs* baseline contrast. The color bar indicates the corresponding T-values. The far-right sagittal plane image displays the slice locations. The upper panel shows results from the ASC group, while the lower panel shows results from the NT group.
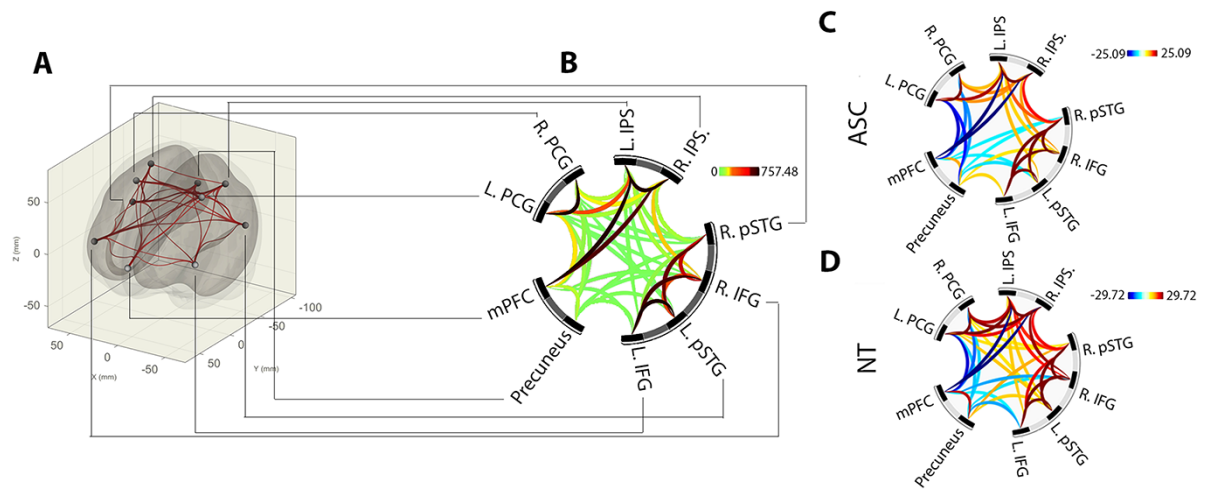
Fig. 3. Overview of connectivity patterns within the network of interest (i.e. AON). A provides a visualization of the regions of interest within the brain, and how they are connected. The specific connections and connectivity strengths are depicted in B, which shows the connectivity ring for the two groups combined, providing a general overview of task-related connectivity. C depicts the same connectivity ring for the ASC group, while D depicts the connectivity ring for the NT group. In B, C, and D, FDR-corrected significant connections are depicted by bands between regions, with band color depicting the F-value (i.e. association between connectivity strength and video viewing condition) for that connection.

the activation of the right IFG (BA 9 and 46), as well as the caudate nucleus. A complete overview of these main results can be seen in Table 2. Figure 2 shows main effects pooled across both groups. No significant clusters were found for the contrasts ASC > NT or NT > ASC.

Connectivity

Our connectivity analyses focused on a network of task-relevant action observation regions (Figure 3A and B). Both groups showed patterns of significant connectivity (Figure 3C and D).

In terms of global efficiency, our linear mixed effects model showed an overall association between participant group and global efficiency, χ^2 (1) = 5.557, P = 0.018. Specifically, this model indicated that global efficiency scores in the NT group were 0.021 higher compared to the ASC group (t = 2.378). However, Tukey-corrected pairwise comparisons across the ROIs revealed no individually significant comparisons, suggesting that while global efficiency for the AON is higher overall in the NT group, the effect may be subtle at the level of individual ROIs. See Figure 4 for an overview of the data distributions.

In terms of local efficiency, we first scaled the values due to model convergence issues. Our linear mixed effects model showed an overall association between the participant group and local efficiency, χ^2 (1) = 5.436, P = 0.019. Specifically, this model indicated that local efficiency scores were 0.483 higher in ASC participants compared to NT participants (t = 2.470). Pairwise comparisons showed higher local efficiency for the left IFG (t-ratio = 2.129, P = 0.035), the left pSTG (t-ratio = 2.473, P = 0.015), the right pSTG (t-ratio = 1.985, P = 0.049) and the overall network (t-ratio = 2.075, P = 0.041). See Figure 5 for an overview of these results.

Association between connectivity and gesture recognition

We did not find any evidence for local efficiency explaining any additional variance in gesture recognition accuracy, χ^2 (4) = 5.054, P = 0.282, or RT, χ^2 (2) = 0.059, P = 0.971, beyond group and kinematic information.

We similarly did not find any evidence for global efficiency explaining any additional variance in gesture recognition accuracy, χ^2 (4) = 4.380, P = 0.357, or RT, χ^2 (2) = 4.365, P = 0.113, beyond group and kinematic information.

## Association between connectivity and neuropsychological measures

For local efficiency, we found no association with AQ (χ^2 (1) = 2.575, P = 0.109) or AFQ (χ^2 (1) = 2.263, P = 0.133). However, we found that local efficiency is associated with motor coordination (χ^2 (1) = 5.616, P = 0.018), with lower efficiency being associated with higher motor coordination (β = −0.066, t = −2.394). See Figure 6A adding Group did not significantly improve the model fit (χ^2 (2) = 2.747, P = 0.253). None of these models contained random slopes. Together these results indicate that local efficiency is significantly associated with motor cognition in general, but group membership does not explain any additional variance in that association.

For global efficiency, we found a significant association with AQ (χ^2 (1) = 4.594, P = 0.032), with lower efficiency scores being associated with higher AQ scores (β = −0.001, t = −2.179, P = 0.036; Figure 6C). Adding Group did not significantly improve the model fit (χ^2 (2) = 1.979, P = 0.372). We additionally found a significant association between global efficiency and motor coordination (χ^2 (1) = 7.059, P = 0.008), with higher global efficiency being associated with higher motor coordination (β = 0.008, t = 2.712, P = 0.010 Figure 6B). Adding Group did not significantly improve the model fit (χ^2 (2) = 3.051, P = 0.218). We found no association between global efficiency and AFQ score (χ^2 (1) = 1.797, P = 0.180). None of these models contained random slopes. Together, these results indicate that global efficiency is associated with both AQ and motor coordination, although group membership does not explain any additional variance in that association.

Discussion

This study set out to quantify differences in brain network topology in autistic and neurotypical individuals during a silent gesture
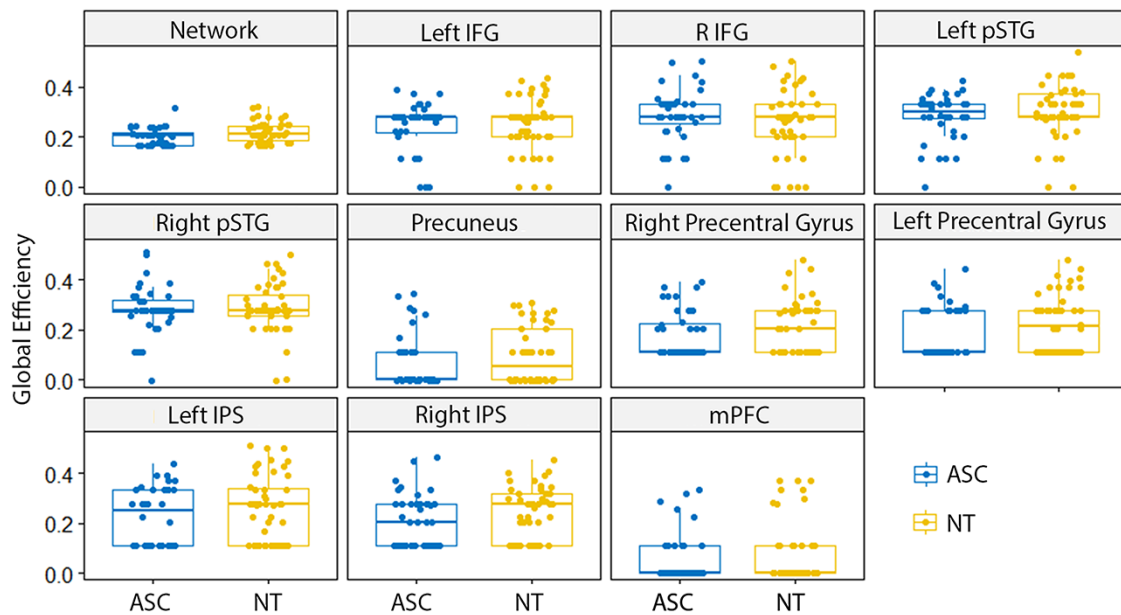
Fig. 4. Global Efficiency, compared between groups, across regions of interest. Each plot represents one of the regions of interest, with the first plot, 'Network', depicting the entire functional network of regions. In each plot, the ASC group is depicted in blue, while the NT group is depicted in yellow. Boxplots depict the global efficiency (y-axis), with the horizontal bar providing the median, the ends of the box providing the first and third quartile. Note that while efficiency is a continuous variable, the possible values it can assume are dependent on the number of connections in a set network. Therefore, the number of unique values can vary per region.
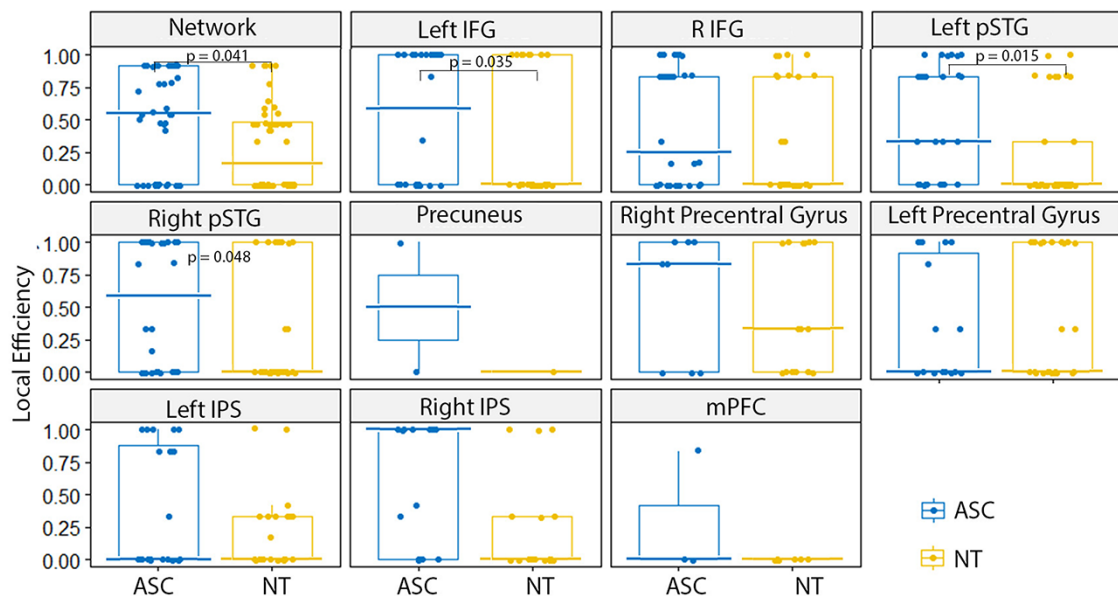

Fig. 5. Local efficiency, compared between groups, across regions of interest. Each plot represents one of the regions of interest, with the first plot, 'Network', depicting the entire functional network of regions. In each plot, the ASC group is depicted in blue, while the NT group is depicted in yellow. Boxplots depict the global efficiency (y-axis), with the horizontal bar providing the median, the ends of the box providing the first and third quartile. Note that while efficiency is a continuous variable, the possible values it can assume are dependent on the number of connections in a set network. Therefore, the number of unique values can vary per region.

recognition task. We found that the AON in autistic individuals was characterized by higher local efficiency and lower global efficiency compared to the AON in the neurotypicals. These findings suggest that functional brain networks organize differently in autistic and neurotypical individuals when viewing and recognizing meaningful (silent) gestures.

In terms of brain activation, both groups showed the activation of areas that are frequently associated with action or gesture processing, including the bilateral IFG. This region has been associated with semantic processing of gestures (Willems *et al.*, 2007; Drijvers *et al.*, 2018), as well as action understanding more generally (Pobric and Hamilton, 2006). We found no significant differences between the two groups in terms of activation, which suggests that any processing differences are more related to the 'organization' of the functional brain network rather than the activation of any particular regions.
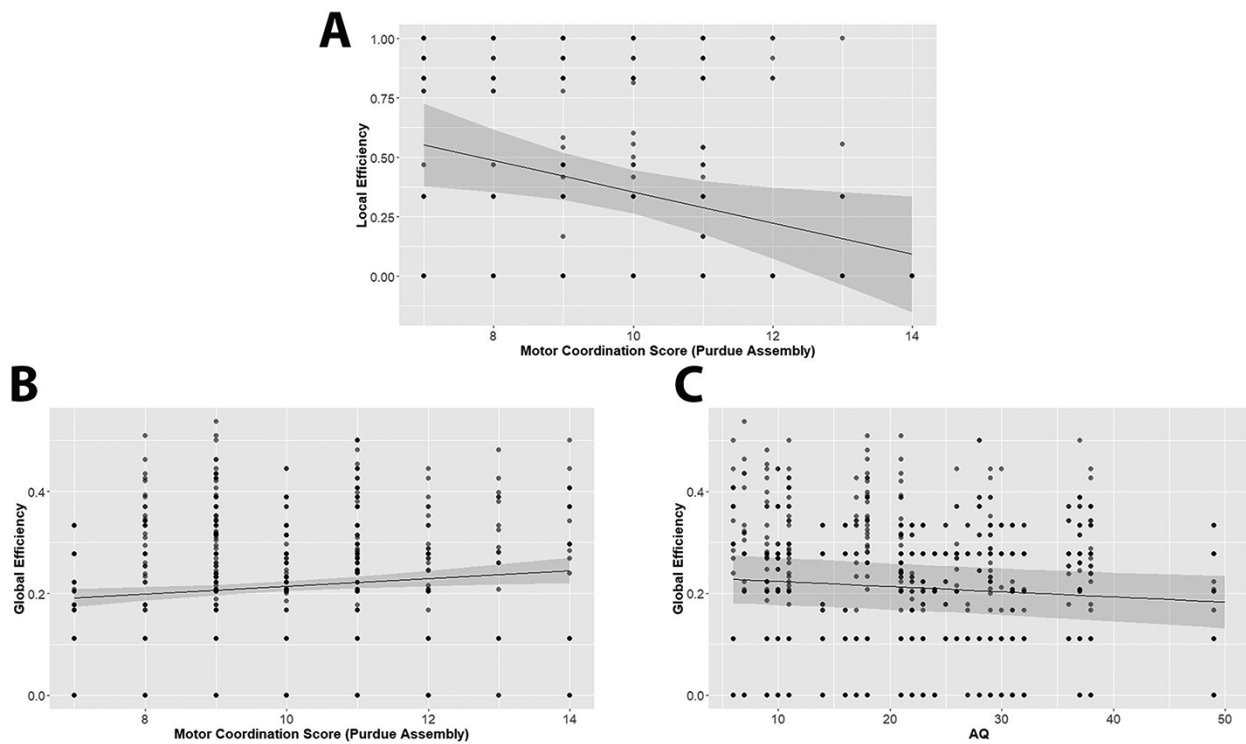
Fig. 6. Significant associations between connectivity measures and behavioral measures. Panel A shows the negative correlation between motor coordination (x-axis) and local efficiency (y-axis). Panel B shows the positive correlation between motor coordination (x-axis) and global efficiency (y-axis). Panel C shows the negative correlation between AQ (x-axis) and global efficiency (y-axis). All panels display the raw data points as circles, and the fit line based on the mixed effects models. The light shading around the fit line provides the standard error of the regression line.

Zooming in to the organization of the AON, we found a dissociation between autistic and neurotypical individuals in terms of how the AON organized during the viewing of communicative gestures. Specifically, autistic individuals showed stronger patterns of local processing than neurotypical individuals, while the neurotypical group conversely showed stronger patterns of global processing. In other words, the AON of autistic individuals shows more characteristics of being segregated. That is, each node (i.e. task-relevant brain region) is more strongly connected to its immediate neighbors rather than more distant regions across the network. This is in contrast to the neurotypical group, where nodes showed comparatively more long-range connections (within the context of the network) rather than being primarily connected with neighboring regions. Most directly, this result fits with the finding of decreased long-range connectivity in autistic individuals during rest (O'Reilly *et al.*, 2017; Hong *et al.*, 2019). This group difference also demonstrates that reduced long-range connectivity also characterizes the brain during gesture recognition. However, it should be noted that the significantly higher global efficiency in the neurotypical group was quite small (0.021 times higher), and it is, therefore, difficult to say if this difference would be meaningful at a behavioral level. Our findings furthermore fit with the general pattern of altered connectivity of the AON in autism (Kilroy *et al.*, 2019). It is especially interesting to note that the specific regions that showed the enhanced local processing efficiency were the pSTG and left IFG, both of which have frequently been indicated as relating to understanding (communicative) movements (Giese and Poggio, 2003; Pobric and Hamilton, 2006; de Lange *et al.*, 2008; Jastorff *et al.*, 2009; Dick *et al.*, 2014). Taken together, task-relevant brain regions, as well as the AON as a whole, seem

to show a different pattern of information transfer in autistic individuals.

Associations between brain and behavior

In addition to the main network findings, these findings can also be tentatively related to behavior. First, we found that, across both groups, higher motor coordination scores were associated with the more 'neurotypical' pattern of network efficiency (i.e. lower local efficiency and higher global efficiency). This is in line with, and builds on, the findings of Kilroy and colleagues who found that motor coordination is associated with activation within the AON (Kilroy *et al.*, 2021). Additionally, lower global efficiency was associated with higher AQ scores, which is in line with Delbruck and colleagues' finding of atypical resting-state connectivity within the AON being associated with autism symptom severity (Delbruck *et al.*, 2019). Together, these findings all point toward lower global efficiency and higher local efficiency being linked to autistic characteristics as measured by more general behavioral or neuropsychological measures, such as the AQ or Purdue pegboard test.

Additionally, while the current paper focused on brain network topology, these findings come from a larger study where we also assessed behavioral performance on this gesture recognition task. In our assessment of the behavioral results of this gesture recognition task, we found that, similar to previous studies (e.g. von der Lühe *et al.*, 2016), autistic individuals were not impaired at recognizing the gestures (Trujillo *et al.*, 2021). However, they seemed to process the communicative modulation of complexity or repetitiveness of movements within the gestures differently than neurotypicals (Trujillo *et al.*, 2021). Our current findings do not show any evidence for these task-related performance

measures being associated with the global or local efficiency of the task-relevant network. Together with the AQ and motor coordination results, it, therefore, seems that network properties are different between autistic and neurotypical individuals and that these topological properties may be associated with more general characteristics but not necessarily with the more fine-grained measures of specific task performance. However, the lack of association with task performance may also be due to the fact that the groups did not differ in terms of accuracy overall but only in the interaction between accuracy and observed kinematics. One possible direction for future work is to look into the role of attention in task performance and its relation to network properties.

Limitations

While this study provides a first investigation of network topology in autistic individuals relating to the recognition of communicative manual gestures, results may be affected by the nature of the stimuli. Specifically, participants performed the task primarily as observers tasked with recognizing gestures without any further linguistic or interactional context. This scenario can affect how a person engages with the communicatively intended stimuli, which may also be reflected in brain responses (Schilbach *et al.*, 2013; Fuchs, 2017). However, given the already variable nature of brain networks in autism (Falahpour *et al.*, 2016), we are confident that our study provides a strong first step to understanding the brain dynamics and the role of sensory processing underlying the recognition of communicative behaviors in autism.

It should also be noted that we do not explicitly control for (i.e. factor out) lower-level aspects of processing such as attention and biological motion processing. Therefore, the network structure is likely related to not only gesture recognition but also the lower-level processes involved in gesture recognition.

Finally, there are several left-handed individuals in our sample. While this is unlikely to affect the network-level graph measures, any differences in lateralization may affect the region-level graph measures (e.g. affecting whether the left or right PCG has a higher local or global efficiency). However, the fact that we still find differences between the groups despite this additional variance suggests that our findings are robust.

Conclusions

In sum, our study builds on previous resting-state functional-connectivity studies of autism by showing that network topology while performing a silent iconic gesture recognition task differs from neurotypicals. Specifically, autistic individuals show increased local efficiency and decreased global efficiency, suggesting a more clustered, local-processing-oriented network configuration rather than the more integrative network organization seen in neurotypical participants. Our study, therefore, provides evidence that functional, task-relevant networks are organized differently in autistic adults. These results have implications for understanding differences in how autistic individuals process (social) information, even when behavioral differences may be relatively subtle.

Acknowledgements

Funding

Conflict of interest

The authors declared that they had no conflict of interest with respect to their authorship or the publication of this article.

Supplementary data

Supplementary data is available at *SCAN* online.

References

Alaerts, K., Geerlings, F., Herremans, L., *et al.* (2015). Functional organization of the action observation network in autism: a graph theory approach. *PLoS One*, **10**(8), e0137020.

Alaerts, K., Swinnen, S.P., Wenderoth, N. (2017). Neural processing of biological motion in autism: an investigation of brain activity and effective connectivity. *Scientific Reports*, **7**(1), 5612.

Aldaqre, I., Schuwerk, T., Daum, M.M., Sodian, B., Paulus, M. (2016). Sensitivity to communicative and non-communicative gestures in adolescents and adults with autism spectrum disorder: saccadic and pupillary responses. *Experimental Brain Research*, **234**(9), 2515–27.

Ansuini, C., Cavallo, A., Bertone, C., Becchio, C. (2014). The visible face of intention: why kinematics matters. *Frontiers in Psychology*, **5**, 815.

Ansuini, C., Cavallo, A., Koul, A., D'Ausilio, A., Taverna, L., Becchio, C. (2016). Grasping others' movements: rapid discrimination of object size from observed hand movements. *Journal of Experimental Psychology. Human Perception and Performance*, **42**(7), 918–29.

Arioli, M., Canessa, N. (2019). Neural processing of social interaction: coordinate-based meta-analytic evidence from human neuroimaging studies. *Human Brain Mapping*, **40**(13), 3712–37.

Baron-Cohen, S., Wheelwright, S., Skinner, R., Martin, J., Clubley, E. (2001). The autism-spectrum quotient (AQ): evidence from asperger syndrome/high-functioning autism, malesand females, scientists and mathematicians. *Journal of Autism and Developmental Disorders*, **31**(1), 5–17.

Bassett, D.S., Meyer-Lindenberg, A., Achard, S., Duke, T., Bullmore, E. (2006). Adaptive reconfiguration of fractal small-world human brain functional networks. *Proceedings of the National Academy of Sciences*, **103**(51), 19518–23.

Blake, R., Turner, L.M., Smoski, M.J., Pozdol, S.L., Stone, W.L. (2003). Visual recognition of biological motion is impaired in children with autism. *Psychological Science*, **14**(2), 151–7.

Bölte, S., Holtmann, M., Poustka, F., Scheurich, A., Schmidt, L. (2007). Gestalt perception and local-global processing in high-functioning autism. *Journal of Autism and Developmental Disorders*, **37**(8), 1493–504.

Bullmore, E., Sporns, O. (2009). Complex brain networks: graph theoretical analysis of structural and functional systems. *Nature Reviews Neuroscience*, **10**(3), 186–98.

Caspers, S., Zilles, K., Laird, A.R., Eickhoff, S.B. (2010). ALE meta-analysis of action observation and imitation in the human brain. *NeuroImage*, **50**(3), 1148–67.

Cohen, J.R., D'Esposito, M. (2016). The segregation and integration of distinct brain networks and their relationship to cognition. *Journal of Neuroscience*, **36**(48), 12083–94.

de Lange, F.P., Spronk, M., Willems, R.M., Toni, I., Bekkering, H. (2008). Complementary systems for understanding action intentions. *Current Biology*, **18**(6), 454–7.

Delbruck, E., Yang, M., Yassine, A., Grossman, E.D. (2019). Functional connectivity in ASD: atypical pathways in brain networks supporting action observation and joint attention. *Brain Research*, **1706**, 157–65.

Desikan, R.S., Ségonne, F., Fischl, B., *et al.* (2006). An automated labeling system for subdividing the human cerebral cortex on MRI scans into gyral based regions of interest. *NeuroImage*, **31**(3), 968–80.

Dick, A.S., Mok, E.H., Beharelle, A.R., Goldin-Meadow, S., Small, S.L. (2014). Frontal and temporal contributions to understanding the iconic co-speech gestures that accompany speech. *Human Brain Mapping*, **35**(3), 900–17.

Drijvers, L., Özyürek, A., Jensen, O. (2018). Hearing and seeing meaning in noise: alpha, beta, and gamma oscillations predict gestural enhancement of degraded speech comprehension. *Human Brain Mapping*, **39**(5), 2075–87.

Enrici, I., Adenzato, M., Cappa, S., Bara, B.G., Tettamanti, M. (2010). Intention processing in communication: a common brain network for language and gestures. *Journal of Cognitive Neuroscience*, **23**(9), 2415–31.

Falahpour, M., Thompson, W.K., Abbott, A.E., *et al.* (2016). Underconnected, but not broken? Dynamic functional connectivity MRI shows underconnectivity in autism is linked to increased intra-individual variability across time. *Brain Connectivity*, **6**(5), 403–14.

Farahani, F.V., Karwowski, W., Lighthall, N.R. (2019). Application of graph theory for identifying connectivity patterns in human brain networks: a systematic review. *Frontiers in Neuroscience*, **13**, 585.

Fishman, I., Keown, C.L., Lincoln, A.J., Pineda, J.A., Müller, R.-A. (2014). Atypical cross talk between mentalizing and mirror neuron networks in autism spectrum disorder. *JAMA Psychiatry*, **71**(7), 751–60.

Fishman, I., Datko, M., Cabrera, Y., Carper, R.A., Müller, R.-A. (2015). Reduced integration and differentiation of the imitation network in autism: a combined functional connectivity magnetic resonance imaging and diffusion-weighted imaging study. *Annals of Neurology*, **78**(6), 958–69.

Fuchs, T. (2017). *Ecology of the Brain: The Phenomenology and Biology of the Embodied Mind*. Oxford, UK: Oxford University Press.

Giese, M.A., Poggio, T. (2003). Neural mechanisms for the recognition of biological movements. *Nature Reviews Neuroscience*, **4**(3), 179–92.

Gießing, C., Thiel, C.M., Alexander-Bloch, A.F., Patel, A.X., Bullmore, E.T. (2013). Human brain functional network changes associated with enhanced and impaired attentional task performance. *Journal of Neuroscience*, **33**(14), 5903–14.

Hendriks, M.P.H., Kessels, R.P.C., Gorissen, M.E.E., Schmand, B.A., Duits, A.A. (2014). *Neuropsychologische diagnostiek: De klinische praktijk*. Amsterdam: Boom.

Herrington, J.D., Baron-Cohen, S., Wheelwright, S.J., *et al.* (2007). The role of MT+/V5 during biological motion perception in asperger syndrome: an fMRI study. *Research in Autism Spectrum Disorders*, **1**(1), 14–27.

Holler, J., Levinson, S.C. (2019). Multimodal language processing in human communication. *Trends in Cognitive Sciences*, **23**(8), 639–52.

Hong, S.-J., Vos de Wael, R., Bethlehem, R.A.I., *et al.* (2019). Atypical functional connectome hierarchy in autism. *Nature Communications*, **10**(1), 1022.

Hsiung, E.-Y., Chien, S.H.-L., Chu, Y.-H., Ho, M.W.-R. (2019). Adults with autism are less proficient in identifying biological motion actions portrayed with point-light displays. *Journal of Intellectual Disability Research*, **63**(9), 1111–24.

Jastorff, J., Kourtzi, Z., Giese, M.A. (2009). Visual learning shapes the processing of complex movement stimuli in the human brain. *Journal of Neuroscience*, **29**(44), 14026–38.

Johansson, G. (1973). Visual perception of biological motion and a model for its analysis. *Perception & Psychophysics*, **14**(2), 201–11.

Keehn, B., Müller, R.-A., Townsend, J. (2013). Atypical attentional networks and the emergence of autism. *Neuroscience and Biobehavioral Reviews*, **37**(2), 164–83.

Kelly, S.D., Özyürek, A., Maris, E. (2010). Two sides of the same coin: speech and gesture mutually interact to enhance comprehension. *Psychological Science*, **21**(2), 260–7.

Ketelaars, C., Horwitz, E., Sytema, S., *et al.* (2008). Brief report: adults with mild autism spectrum disorders (ASD): scores on the autism spectrum quotient (AQ) and comorbid psychopathology. *Journal of Autism and Developmental Disorders*, **38**(1), 176–80.

Kilroy, E., Cermak, S.A., Aziz-Zadeh, L. (2019). A review of functional and structural neurobiology of the action observation network in autism spectrum disorder and developmental coordination disorder. *Brain Sciences*, **9**(4), 75.

Kilroy, E., Harrison, L., Butera, C., *et al.* (2021). Unique deficit in embodied simulation in autism: an fMRI study comparing autism and developmental coordination disorder. *Human Brain Mapping*, **42**(5), 1532–46.

Knoblich, G., Sebanz, N. (2006). The social nature of perception and action. *Current Directions in Psychological Science*, **15**(3), 99–104.

Lakens, D., Scheel, A.M. & Isager, P.M. (2018). Equivalence testing for psychological research: a tutorial. *Advances in Methods and Practices in Psychological Science*, **1**(2), 259–69.

Lawson, R.P., Mathys, C., Rees, G. (2017). Adults with autism overestimate the volatility of the sensory environment. *Nature Neuroscience*, **20**(9), 1293–9.

Lee, P., Liu, C.H., Fan, C.W., *et al.* (2013). The test–retest reliability and the minimal detectable change of the Purdue Pegboard Test in schizophrenia. *Journal of the Formosan Medical Association*, **112**(6), 332–7.

McKay, L.S., Simmons, D.R., McAleer, P., Marjoram, D., Piggot, J., Pollick, F.E. (2012). Do distinct atypical cortical networks process biological motion information in adults with autism spectrum disorders? *NeuroImage*, **59**(2), 1524–33.

Mumford, J.A., Nichols, T.E. (2008). Power calculation for group fMRI studies accounting for arbitrary design and temporal autocorrelation. *NeuroImage*, **39**(1), 261–8.

O'Reilly, C., Lewis, J.D., Elsabbagh, M. (2017). Is functional brain connectivity atypical in autism? A systematic review of EEG and MEG studies. *PLoS One*, **12**(5), e0175870.

Özyürek, A. (2014). Hearing and seeing meaning in speech and gesture: Insights from brain and behaviour. *Philosophical Transactions of the Royal Society B: Biological Sciences*, **369**(1651), 20130296.

Park, H.-J., Friston, K. (2013). Structural and functional brain networks: from connections to cognition. *Science*, **342**(6158), 1238411.

Peirce, J.W., Gray, J.R., Simpson, S., *et al.* (2019). PsychoPy2: experiments in behavior made easy. *Behavior Research Methods*, **51**, 195–203.

Pellicano, E., Burr, D. (2012). When the world becomes 'too real': a Bayesian explanation of autistic perception. *Trends in Cognitive Sciences*, **16**(10), 504–10.

Pobric, G., Hamilton, A.F.D.C. (2006). Action understanding requires the left inferior frontal cortex. *Current Biology*, **16**(5), 524–9.

Rolls, E.T., Huang, C.-C., Lin, C.-P., Feng, J., Joliot, M. (2020). Automated anatomical labelling atlas 3. *NeuroImage*, **206**, 116189.

Rorden, C., Brett, M. (2000). Stereotaxic display of brain lesions. *Behavioural Neurology*, **12**(4), 191–200.

Sapey-Triomphe, L.-A., Timmermans, L., Wagemans, J. (2020). Priors bias perceptual decisions in autism, but are less flexibly adjusted to the context. *Autism Research*, **14**(6), 1134–46.

Schilbach, L., Timmermans, B., Reddy, V., *et al.* (2013). Toward a second-person neuroscience. *The Behavioral and Brain Sciences*, **36**(4), 393–414.

Silverman, L.B., Bennetto, L., Campana, E., Tanenhaus, M.K. (2010). Speech-and-gesture integration in high functioning autism. *Cognition*, **115**(3), 380–93.

Tettamanti, M., Vaghi, M.M., Bara, B.G., Cappa, S.F., Enrici, I., Adenzato, M. (2017). Effective connectivity gateways to the Theory of Mind network in processing communicative intention. *NeuroImage*, **155**, 169–76.

Tiffin, J., Asher, E.J. (1948). The purdue pegboard: norms and studies of reliability and validity. *Journal of Applied Psychology*, **32**(3), 234–47.

Todorova, G.K., Hatton, R.E.M., Pollick, F.E. (2019). Biological motion perception in autism spectrum disorder: a meta-analysis. *Molecular Autism*, **10**(1), 49.

Trujillo, J.P., Simanova, I., Bekkering, H., Özyürek, A. (2018). Communicative intent modulates production and comprehension of actions and gestures: a kinect study. *Cognition*, **180**, 38–51.

Trujillo, J.P., Vaitonyte, J., Simanova, I., Özyürek, A. (2019). Toward the markerless and automatic analysis of kinematic features: a toolkit for gesture and movement research. *Behavior Research Methods*, **51**(2), 769–77.

Trujillo, J.P., Simanova, I., Ozyurek, A., Bekkering, H. (2020). Seeing the unexpected: how brains read communicative intent through kinematics. *Cerebral Cortex*, **3**(30), 1056–67.

Trujillo, J.P., Özyürek, A., Kan, C.C., Sheftel-Simanova, I., Bekkering, H. (2021). Differences in the production and perception of communicative kinematics in autism. *Autism Research*, **14**, 2640–53.

Van de Cruys, S., Evers, K., Van der Hallen, R., *et al.* (2014). Precise minds in uncertain worlds: predictive coding in autism. *Psychological Review*, **121**(4), 649.

Van de Cruys, S., Van der Hallen, R., Wagemans, J. (2017). Disentangling signal and noise in autism spectrum disorder. *Brain and Cognition*, **112**, 78–83.

van der Meer, H.A., Sheftel-Simanova, I., Kan, C.C., Trujillo, J.P. (2022). Translation, cross-cultural adaptation, and validation of a Dutch version of the actions and feelings questionnaire in autistic and neurotypical adults. *Journal of Autism and Developmental Disorders*, **52**, 1771–7.

van Ool, J.S., Hurks, P.P., Snoeijen-Schouwenaars, F.M., *et al.* (2018). Accuracy of WISC-III and WAIS-IV short forms in patients with neurological disorders. *Developmental Neurorehabilitation*, **21**(2), 101–7.

Verhage, F. (1964). *Intelligentie en leeftijd: Onderzoek bij Nederlanders van twaalf tot zevenenzeventig jaar [Intelligence and Age: Research in Dutch Persons Age Twelve to Seventy-seven Years]*. The Netherlands: van Gorcum, Groningen.

Villarreal, M., Fridman, E.A., Amengual, A., *et al.* (2008). The neural substrate of gesture recognition. *Neuropsychologia*, **46**(9), 2371–82.

von der Lühe, T., Manera, V., Barisic, I., Becchio, C., Vogeley, K., Schilbach, L. (2016). Interpersonal predictive coding, not action perception, is impaired in autism. *Philosophical Transactions of the Royal Society B: Biological Sciences*, **371**(1693), 20150373.

Walther, S., Stegmayer, K., Sulzbacher, J., *et al.* (2015). Nonverbal social communication and gesture control in schizophrenia. *Schizophrenia Bulletin*, **41**(2), 338–45.

Wechsler, D. (2011). *WASI-II: Wechsler Abbreviated Scale of Intelligence*. San Antonio, TX, USA: Psychological Corporation.

Willems, R.M., Özyürek, A., Hagoort, P. (2007). When language meets action: the neural integration of gesture and speech. *Cerebral Cortex*, **17**(10), 2322–33.

Williams, J.H.G., Cameron, I.M., Ross, E., Braadbaart, L., Waiter, G.D. (2016). Perceiving and expressing feelings through actions in relation to individual differences in empathic traits: the action and feelings questionnaire (AFQ). *Cognitive, Affective & Behavioral Neuroscience*, **16**(2), 248–60.

World Medical Association. (2013). World medical association declaration of Helsinki: ethical principles for medical research involving human subjects. *JAMA*, **310**(20), 2191–4.

Appendix 1. Gesture items

Original (Dutch)	Response option Dutch	English	Response option English
doe de apple in de kom	Plaatsen	Place the apple in the bowl	Place
borstel je haar met de borstel	Borstelen	Brush your hair with the brush	Brush
veeg het papier af	Afvegen	Brush off the paper	Brush off
kreukel het papier	Kreukelen	Crumple the paper	Crumple
snij het brood met de mes	Snijden	Cut the bread with the knife	Cut
knip het papier doormidden	Knippen	Cut the paper in half	Cut
wis de figuur met de gom	Wissen	Erase the figure with the eraser	Erase
vouw het papier doormidden	Vouwen	Fold the paper in half	Fold
sla de spijkers met de hammer	Hameren	Hammer the nails with the hammer	Hammer
meet het papier met het meetlint	Meten	Measure the paper with the measuring tape	Measure
open het potje	Opendoen	Open the jar	Open
open het slot met de sleutel	Openmaken	Open the lock with the key	Open
pel de banaan	Pellen	Peel the banana	Peel
doe het dopje op de pen	Opdoen	Put the pencap on the pen	Put on
giet het water in het glas	Gieten	Pour the water in the glass	Pour
doe de hoed op	Opdoen	Put on the hat	Put on
doe de ring aan	Aandoen	Put on the ring	Put on
verwijder het kurkje van de fles	Verwijderen	Remove the cork from the bottle	Remove
verwijder het dopje van de pen	Verwijderen	Remove the pencap from the pen	Remove
schrob het bureau met de spons	Schrobben	Scrub the desk with the sponge	Scrub
schud de kaarten door elkaar	Schudden	Shuffle the cards	Shuffle
pers de citroen uit	Persen	Squeeze the lemon	Squeeze
stapel de blokken op elkaar	Stapelen	Stack the blocks on top of each other	Stack
stempel het papier	Stempelen	Stamp the paper	Stamp
niet de papieren samen	Nieten	Staple the papers together	Staple
dompel het theezakje in het water	Dompelen	Steep the teabag in the water	Steep
roer de thee met de lepel	Roeren	Stir the tea with the spoon	stir
doe de zonnebril op	Opdoen	Put on the sunglasses	Put on
scheur het papier doormidden	Scheuren	Tear the paper in half	Tear
gooi de dobbelstenen	Gooien	Roll the dice	Roll (throw)
schrijf je naam op het papier met de pen	Schrijven	Write your name on the paper with the pen	write

Appendix 2. Behavioral results

	% Accuracy (s.d.)	RT in milliseconds (s.d.)
ASC	69.95 (12.4)	1439.49 (576.7)
NT	71.14 (5.2)	1132.83 (295.5)